Efficient Performance Evaluation for Multistatic SAR Systems

Nida Sakar*, Pau Prats-Iraola, Marc Rodriguez-Cassola

*German Aerospace Center, Microwaves and Radar Institute Muenchner Str. 20, 82234 Wessling, GERMANY
email: nida.sakar@dlr.dr

Abstract: *In this paper, we present an efficient azimuth reconstruction performance evaluation strategy for multi-aperture Synthetic Aperture Radar (SAR) systems. The goal is to evaluate the quality metrics of a focused impulse response function without having to perform a costly point-target simulation followed by an azimuth reconstruction and focusing. This methodology is convenient especially for multi-static SAR systems where the baseline between the receivers and the transmitter, i.e. the sampling condition, changes dynamically, and a Monte-Carlo based performance evaluation is necessary.*

1. Introduction

Spaceborne SAR systems have become an irreplaceable source of information for the scientific community over the past three decades due to its wide range of practical applications. A thorough understanding of Earth's dynamic processes requires systematic high-resolution imaging with short temporal baselines. Conventional SAR systems fail to comply with the requirements on the resolution and temporal baseline simultaneously, and can only offer one at the expense of the other. Therefore, next-generation spaceborne SAR systems aim at fulfilling this demanding requirement via advanced imaging and signal processing techniques. Multi-aperture SAR systems make use of several transmit and receive channels for boosting the performance of the system. Such a concept with one transmit and multiple receive units can be utilized for high-resolution wide-swath (HRWS) imaging and/or reducing the antenna length with digital beamforming in azimuth. The usage of multi-aperture architectures in azimuth and digital beamforming techniques are the present-day center of interest for the next-generation HRWS satellite missions, such as the Radar Observing System for Europe at L-band (ROSE-L) mission of the Copernicus Expansion Programme. Exchanging the complex and large monostatic SAR satellites with a constellation of small, simple and less expensive ones is another popular research topic, which is currently under investigation for ESA's Distributed SAR for Space 4.0 (DistSAR-4.0) project.

In such systems, the performance evaluation model is usually raw-data based, where the time-domain simulation of point targets is followed by the azimuth reconstruction and focusing. This methodology is computationally expensive for the constellation analysis and limits the number of mission scenarios that can be evaluated. However, it is essential to validate the system performance efficiently for all possible scenarios, e.g., different pulse repetition interval (PRI)

978-3-944976-34-1

schemes (constant, periodically varying, random), constellation sizes, swath widths, in order to determine the system parameters for a robust multi-aperture SAR system. This paper presents a methodology to quantify the performance of a azimuth reconstruction algorithm without having to perform a computationally expensive point-target simulation. The methodology is based on the computation of the azimuth reconstruction filters in the Doppler-domain [1], hence, the PRI variation options are limited to constant and periodically varying. Nevertheless, as already shown in [2], the impact of a varying PRI can be characterized accurately by a periodically varying PRI (linear PRI variation).

2. Multi-aperture Along-track SAR Configurations

An along-track multi-aperture SAR (SIMO) system consists of one transmitter and N_{rx} receive antennas. These transmit/receive units are either on a single platform or on separate platforms flying on the same orbit each with an along-track baseline of b_i. As a rule of thumb, all of these receive and transmit units should illuminate the same area on the ground. The additional receive units of single-platform systems can be obtained by splitting the transmit antenna (physically or electronically) in azimuth when receiving. In the multi-platform case, the receive units are equipped with passive radar antennas. Figure 1 illustrates these two possible realizations of a multi-aperture SAR concept. ROSE-L is an example of a single platform multi-channel system, where the mission scenarios considered for the DistSAR-4.0 falls into the multi platform case.

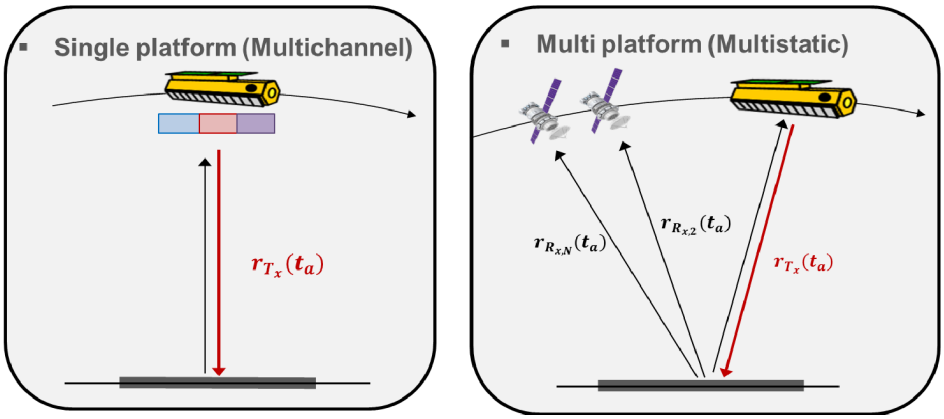

Figure 1: Multi-aperture SAR system in azimuth: (left) single platform and (right) multi platform..

The technique keeps the operational pulse repetition frequency (PRF) below the Nyquist criterion by a factor called system scaling η_{ss} aiming at relaxing the constraint on the non-ambiguous swath width,

$$PRF \geq \frac{B_a}{\eta_{ss}}, \tag{1}$$

where B_a is the Doppler bandwidth. The available sampling and the effective sampling of the system are increased by the number of available satellites $PRF \cdot N_{rx}$ and of the system scaling

$PRF \cdot \eta_{ss}$, respectively, where $N_{rx} = (1 + \alpha) \cdot \eta_{ss} \geq \eta_{ss}$. Note that depending on the mission concept, the active sensor can be operated in transmit-and-receive mode or solely in transmit mode. In such a system, since the echoes of the individual receivers appear strongly aliased, the recovery of the Doppler spectrum via reconstruction is required to increase the effective sampling before the SAR image formation occurs. Numerous methods for multi-channel/multistatic azimuth reconstruction exist in the literature [3, 4, 6, 5]. In the following sections, we evaluate and compare the performance of the inverse filter [3] and optimum filter [4], i.e., Minimum Variance Distortionless Response (MVDR) filter.

The main drawback of multi-static SAR systems is the dynamically changing sampling condition due to the receivers' movement in the orbital tube. The sampling condition plays a fundamental role in the successful retrieval of the unambiguous Doppler bandwidth and consequent suppression of azimuth ambiguities. Controlling the along-track position of the receivers within one resolution period of the reconstructed signal is sufficient for ensuring the absence of coinciding samples. Nevertheless, this requirement becomes stringent for higher frequencies and very high resolutions. Increasing the sampling rate of the constellation, either by raising the PRF of operation or by the use of a larger number of receive satellites can improve the sampling condition. In [2], we investigated the impact of the varying PRI schemes and orbit control accuracy on the azimuth reconstruction performance with the point-target based Monte-Carlo approach, which is computationally expensive. An efficient azimuth reconstruction performance methodology is more convenient to quantify the impacts of all relevant aspects on the azimuth reconstruction performance and determine system parameters including the size of the constellation, i.e., the oversampling factor in terms of receivers (α).

3. Evaluation of the Azimuth Reconstruction Performance

A generalized performance evaluation methodology for an azimuth reconstruction needs to be capable of accommodating dynamically varying baselines and different PRI schemes. The left plot of Figure 2 shows the block diagram of the raw-data based performance evaluation method. After setting the baselines (randomly) and the PRI scheme, corresponding orbits and raw data are generated. For the systems with a constant or periodically varying PRI schemes, a Doppler-domain azimuth reconstruction takes place due to its efficiency. The time-domain reconstruction algorithm suggested in [2] needs to be used for the randomly varying PRI schemes. Afterwards, the data are focused and performance parameters, namely, Azimuth-Ambiguity-to-Signal Ratio (AASR), noise scaling and sensitivity to channel imbalances, are computed. Finally, the performance characterization is done by computing the $1 - 3\sigma$ percentiles.

The right plot of Figure 2 shows the block diagram of the efficient reconstruction-filter based performance evaluation method. This approach skips most of the processing steps and only requires the computation of the reconstruction filters, which is a part of the azimuth reconstruction step in the raw-data based method. Additionally, the number of the azimuth samples is independent of the resolution and the acquisition time of the simulation (number of the spectral copies of the Doppler bandwidth), hence, that leads to less computational time. As mentioned before,

this methodology is not suitable for irregular PRI schemes. In the following, the computation of the performance parameters for both methodologies are explained.

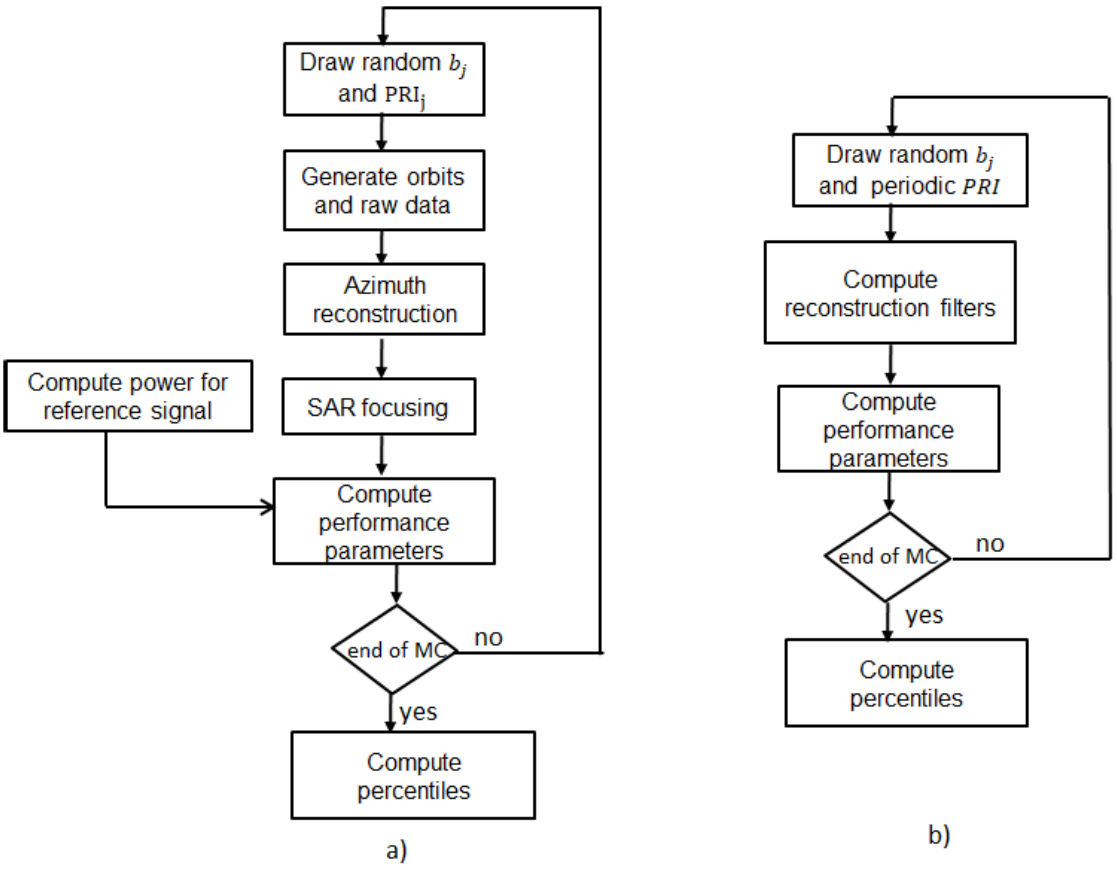

Figure 2: Azimuth reconstruction performance evaluation block diagram a) conventional raw-data based b) efficient reconstruction-filter based.

3.1. Azimuth-Ambiguity-to-Signal Ratio

In the case of multi-aperture systems in along-track, azimuth ambiguities are caused by the energy outside of the reconstructed baseband and the mismatch in the reconstruction process, which might be coming from sampling condition, baseline knowledge, topography, residual instrument errors, etc. The computation of AASR must be suitable for both constant PRI and varying PRI schemes. In case of a raw-data based methodology, AASR is computed from the simulated data as defined in [8], i.e.,

$$\mathrm{AASR} = 10\log_{10}\left(\frac{p_{sl} - p_{sl,ref}}{p_{ml}}\right) \tag{2}$$

where p_{sl} and p_{ml} are the sidelobe and mainlobe power, respectively, and $p_{sl,ref}$ is the sidelobe power for an ideal response. The reason for that is the ambiguities of the systems with a varying PRI scheme appear in the image as a noise-like disturbance. In case of the efficient methodology,

AASR can be estimated from the receivers' transfer functions and the reconstruction filters as [1]

$$\text{AASR} = 10\log_{10}\left(\frac{p_t - p_s}{p_s}\right) \tag{3}$$

$$p_t(f_a) = 2 \cdot \sum_{k=1}^{\infty}\left(A_k(f_a)\sum_{m=1}^{N_{rx}}\sum_{j=1}^{N_{rx}}|H_{jk}(f_a)\cdot P_{jm}(f_a)|^2\right) \tag{4}$$

where p_t is the total power, p_s is the signal power, A_k is the antenna pattern, H_{jk} is the transfer function for the receiver j within the k-th continuation of the original spectrum and P_{jm} is the reconstruction filter for the sub-band m of the receiver j.

3.2. Noise Scaling

The reconstruction filters aim at suppressing the unwanted frequency component by putting them to zeros and retrieving the aliasing-free Doppler bandwidth. Once a multi-aperture system diverts from uniform sampling case, the reconstruction algorithm cannot cancel out all of the unwanted components, which consequently increases the noise floor, resulting in loss of signal energy and worse signal-to-noise ration (SNR). The conventional way of evaluating the noise scaling is done numerically with a Monte-Carlo by applying reconstruction filters to the Gaussian white noise and averaging the increase in the noise power after the azimuth reconstruction. An alternative way of computing the noise scaling by using the reconstruction filters as [1]

$$\phi_{bf} = \frac{SNR_{el}/SNR_{out}}{(SNR_{el}/SNR_{out})\Big|_{PRF_{uni}}} = \frac{\sum_{j=1}^{N_{rx}}[|P_j(f_a)|^2]}{N_{rx}}. \tag{5}$$

3.3. Sensitivity to Channel Imbalances

The exact knowledge of the receivers' transfer functions in the multi-aperture systems plays a fundamental role in the performance of the azimuth reconstruction, hence, an adequate channel calibration is necessary. The impact of the channel imbalances shows itself as azimuth ambiguities, and can be computed with the point-target based methodology as described by (2) after ingesting them to the raw data generation. For the efficient methodology, we use (3) by inserting the phase error to the transfer function.

4. Simulation Results

In this section, the azimuth reconstruction performance metrics for ROSE-L satellite are shown, and some preliminary analysis on the replacing Sentinel-1 and Tandem-L satellites with an along-track SAR constellation of small satellites (as a part of DistSAR4.0 study) are presented.

Table 1: ROSE-L system parameters

Wavelength [m]	0.24
PRF [Hz]	1374.55 / 1511.71
Processed BW [Hz]	2200
Number of Rx	5
Slant range [km]	800
Velocity [m/s]	7600
Antenna size [m]	2.2 x 3.6

The system parameters of ROSE-L is very conveniently designed, so that most of the chosen operational PRFs form almost uniform sampling, PRF=1374.55 Hz being the best sampling and PRF=1511.71 Hz being the worst. As mentioned before, the inverse filter and optimum filter are chosen for the azimuth reconstruction performance evaluation. This allows us to compare these two different algorithms and determine the better suited one for the ROSE-L system. The inversion filter is based on a noise-free model that solely focuses on suppressing the ambiguities and includes all of the input data regardless of their sampling condition and noise level, a fact that might reduce the final SNR. On the other hand, the optimum filter suppresses azimuth ambiguities subject to optimizing the SNR with respect to white noise, which may result in poor ambiguity suppression compared to the inverse filter.

Figure 3 shows the impulse response function (IRF) of a reconstructed point target. The raw data simulation is done with the ROSE-L parameters shown in Table 1 and the performance figures are computed with (2) and numerically with a Monte-Carlo simulation. This figure compares the performance of the reconstruction algorithms in hand with respect to each other and illustrates the performance degradation due to the sampling condition. The plots show the azimuth reconstruction with the inverse filter, optimum filter with a correct noise power estimation and optimum filter with an overestimated noise power. As expected, the reconstruction performance of the inverse filter and optimum filter with a correct noise power estimation are the same. On the other hand, additional ambiguities are noticeable (worse ambiguity suppression performance) if the data are reconstructed with the optimum filter with an overestimated noise power (first ambiguities). The outcome of this computationally expensive analysis can be estimated with the filter-based approach as well. Figure 4 shows the AASR estimation with the same simulation parameters. It is evident that the inverse filter and optimum filter perform the same in the uniform sampling case, and the azimuth ambiguity suppression performance of the inverse filter is slightly better if the noise power is overestimated (bottom-right plot).

Figure 5 shows the numerical and analytical estimation of the noise scaling with the same simulation parameters of Figure 3. The numerical noise scaling is estimated via getting the mean value of a Monte-Carlo simulation, where the inverse filter is applied on the Gaussian white noise. Therefore, the analytical noise scaling estimation of the inverse filter is placed in the middle of the numerical estimation. It is clear that the noise scaling of the filters matches if the noise power is estimated correctly and, as expected, the noise scaling of the optimum filter is lower than the inverse filter if the noise power is overestimated. This plot shows that the noise

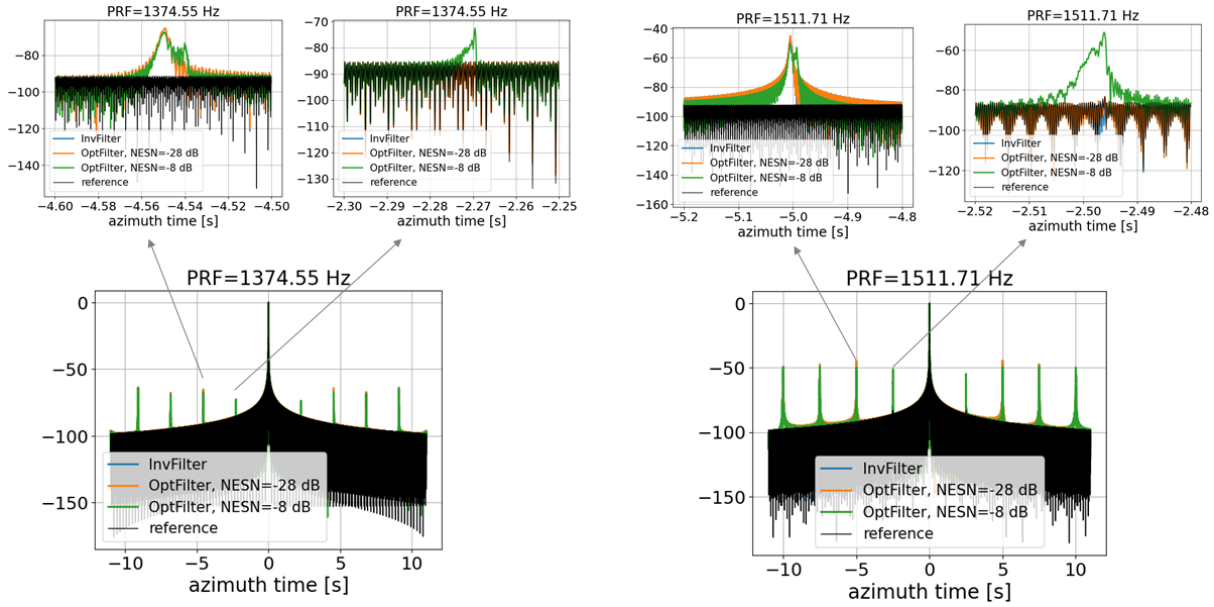

Figure 3: Impulse response function of the reconstructed and focused point target which is simulated by using ROSE-L parameters with the PRFs (left) providing best sampling condition and (right) providing the worst sampling. The top plots show zoomed first and second ambiguities to compare the inverse filter, optimum filter and optimum filter with overestimated noise power.

scaling metric can be accurately estimated by using the reconstruction filters as described in (5).

Figure 6 shows the analytical estimation of AASR with the presence of the channel imbalances. The left plots show the AASR with a channel imbalance of (top) 4° and (bottom) 8° and the right plot shows the mean AASR with respect to the different phase errors. The Monte-Carlo simulation is repeated 1000 times. Simulations indicate that a imbalances should be calibrated with an accuracy better than 2.5° to keep the AASR below -25 dB.

One part of the DistSAR4.0 study investigates the potentials and challenges of replacing complex SAR systems with monostatic and multi-static SAR constellations equipped with small and light weight antennas. Two of the investigated example systems are Sentinel-1 and Tandem-L with the antenna sizes of 12.3 m x 0.821 m (planar) and 15 m (reflector), respectively. The Sentinel-1 can be replaced by a monostatic constellation of five satellites covering one portion of the 250 km swath each with a 9 m x 0.9 m antenna by keeping the resolution constant. Each of the monostatic satellites can be replaced by an along-track multi-static constellation ($N_{rx} >= \eta_{ss} = 9$) each equipped with an 1.1 m x 0.9 m antenna, resulting in better azimuth resolution. On the other hand, the Tandem-L satellite can be replaced by a monostatic constellation of two satellites, each covering the half of the 350 km swath with a 30 m x 1.2 m antenna. Since the antenna area is still quite large, this monostatic constellation can be replaced with an along-track multi-static constellation ($N_{rx} >= \eta_{ss} = 20$) each equipped with an 1.5 m x 1.2 m antenna. Figure 7 shows the AASR and noise scaling with respect to the oversampling factor in terms of receive satellites (α). The dashed black lines in the top plots represents the required AASR for the equivalent systems. For the analysis, a cyclic randomly varying PRI

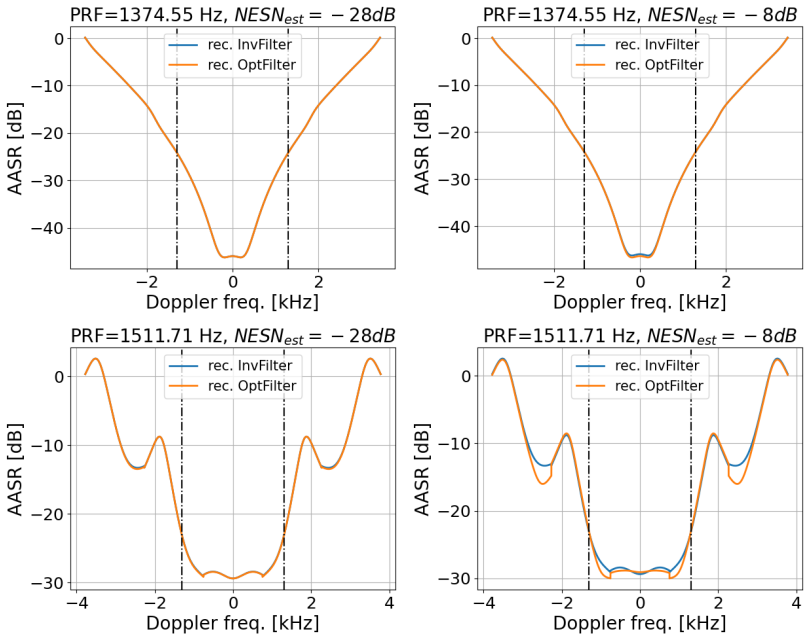

Figure 4: AASR estimation with the efficient reconstruction-filter based method. Top: the best sampling condition, bottom: the worst sampling condition of ROSE-L, left: with the correct noise power estimation, right: with the overestimated noise power. The black dashed lines show the processed bandwidth of 2.6 KHz.

(with an interval of 16) and a constant PRI are considered. It is clear that the AASR and noise scaling values gets better with the larger oversampling factors. As already shown in [2], the tight orbit control provides better performance improvement than the PRI variation. According to the AASR plots, Sentinel-1 can be replaced with five constellations of 22 satellites in case of a varying PRI and 18 satellites in case of a constant PRI. On the other hand, Tandem-L can be replaced with two constellations of 80 satellites in case of a varying PRI and 70 satellites in case of a constant PRI.

5. Summary

This paper presents two azimuth reconstruction performance evaluation methods based on a point-target simulation and azimuth reconstruction filters. An efficient methodology to characterize the performance of a multi-aperture SAR system is beneficial especially for the design of future SAR missions. It can be utilized to determine the constellation size for different mission scenarios (PRI variation, resolution, swath width, wavelength) considering the system requirements and current/future orbit control technology. Additionally, quantifying the impact of the error sources such as sampling condition, baseline knowledge topography, residual instrument errors becomes straightforward for all multi-aperture systems.

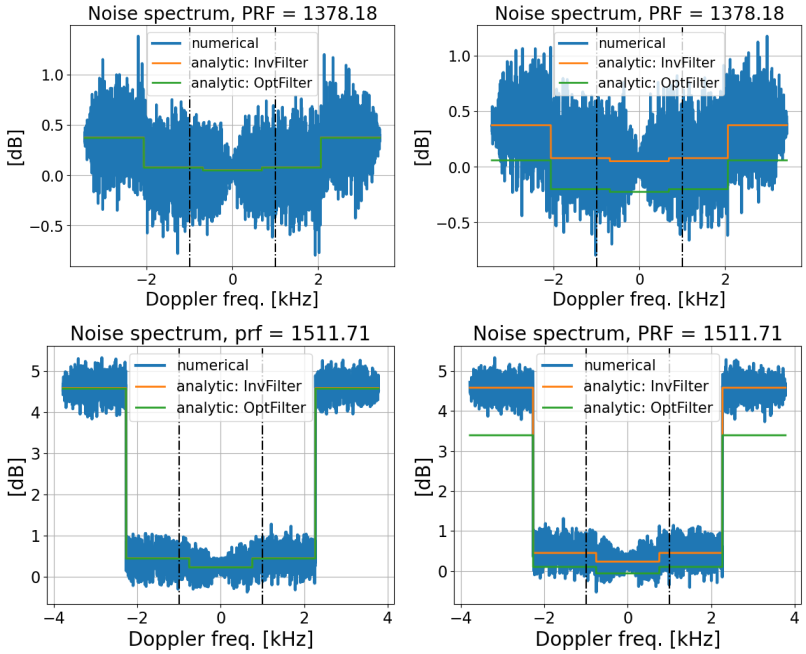

Figure 5: Numerical and analytical noise scaling estimation . Top: the best sampling condition, bottom: the worst sampling condition of ROSE-L, left: with the correct noise power estimation, right: with the overestimated noise power. The black dashed lines show the processed bandwidth of 2.2 KHz.

References

[1] N. Gebert and G. Krieger, and A. Moreira, "Digital Beamforming on Receive: Techniques and Optimization Strategies for High-Resolution Wide-Swath SAR Imaging", *IEEE Transactions on Aerospace and Electronic Systems*, 2010, vol. 45, no. 2, pp. 564-592.

[2] N. Sakar, M. Rodriguez-Cassola, P. Prats-Iraola, and A. Moreira, "Sampling Analysis and Processing Approach for Distributed SAR Constellations with Along-track Baselines", *IEEE Transactions on Geoscience and Remote Sensing*, 2022, vol. 60, pp. 1-12.

[3] G. Krieger, N. Gebert, and A. Moreira, "Unambiguous SAR Signal Reconstruction from Nonuniform Displaced Phase Center Sampling", *IEEE Geoscience and Remote Sensing Letters*, 2004, vol. 1, no. 4, pp. 260-264.

[4] Z. Li, H. Wang, T. Su, and Z. Bao, 'Generation of Wide-Swath and High-Resolution SAR Images from Multichannel Small Spaceborne SAR Systems", *IEEE Geoscience and Remote Sensing Letters*, 2005, vol. 1, no. 1, pp. 82-86.

[5] I. Sikaneta, C. H. Gierull, and D. Cerutti-Maori, 'Optimum Signal Processing for Multichannel SAR: With Application to High-Resolution Wide-Swath Imaging", *IEEE Transactions on Geoscience and Remote Sensing*, 2014, vol. 52, no. 10, pp. 6095-6109.

[6] D. Cerutti-Maori, I. Sikaneta, J. Klare, and C. H. Gierull, "MIMO SAR Processing for Multichannel High-Resolution Wide-Swath Radars", *IEEE Transactions on Geoscience and Remote Sensing*, 2014, vol. 52, no. 8, pp. 5034-5055.

[7] F. Queiroz de Almeida, M. Younis, G. Krieger, and A. Moreira, "An Analytical Error Model for Spaceborne SAR Multichannel Azimuth Reconstruction", *IEEE Geoscience and Remote Sensing Letters*, 2018, vol. 15, no. 6, pp. 853-857.

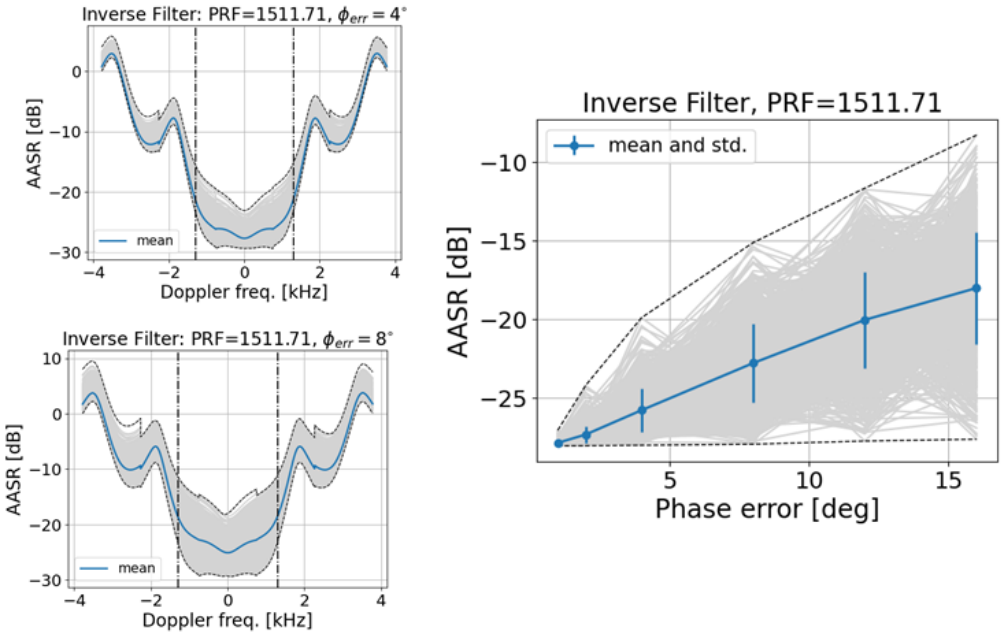

Figure 6: Sensitivity to channel imbalances. Left: AASR estimation for each Doppler frequency bin (top) with a 4° phase error and (bottom) with an 8° phase error, Right: mean value of the Monte-Carlo analysis for different phase errors.

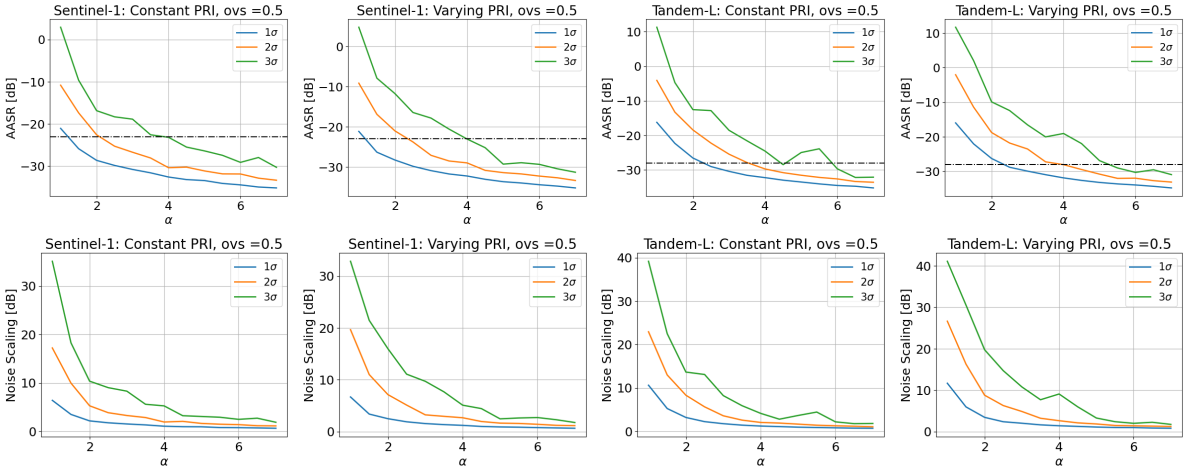

Figure 7: Constellation size analysis based on (top) AASR and (bottom) the noise scaling for replacing the Sentinel-1 and Tandem-L satellites with multi-static along-track constellations. The black dashed lines show the required AASR values in each system and the oversampling factor is set to 0.5.

[8] M. Villano and G. Krieger, and A. Moreira, “Staggered SAR: High-Resolution Wide-Swath Imaging by Continuous PRI Variation”, *IEEE Transactions on Geoscience and Remote Sensing*, 2014, vol. 52, no. 7, pp. 4462-4479.